ELSEVIER

Ceramics International 27 (2001) 325–334

CERAMICS INTERNATIONAL

www.elsevier.com/locate/ceramint

Mg_2SnO_4 ceramics I. Synthesis–processing–microstructure correlation

Abdul-Majeed Azad *, Liew Jing Min

Department of Physics, University Putra Malaysia, 43400 UPM Serdang, Selangor, Malaysia

Received 6 June 2000; received in revised form 18 June 2000; accepted 19 July 2000

Abstract

Phase stability of magnesium meta- and orthostannate has been examined in samples synthesized via the traditional solid-state reaction (SSR) and a novel self-heat-sustained (SHS) technique with two molar ratios of magnesium to tin (viz., 1:1 and 2:1). The powder mixtures were calcined over a wide temperature–time (T–t) span ranging from 600 to 1300°C and 3 to 72 h. The powders obtained from the two preparative methods have been processed and sintered under identical conditions. In the 2:1 molar mixtures, Mg_2SnO_4 has been formed as a single phase up on calcination in both SRR and SHS methods. This phase remained the only compound in the sintered bodies as well. In the 1:1 composition, the ultimate reaction product was a mixture of Mg_2SnO_4 and SnO_2. Both SSR and SHS techniques with 2:1 molar mixture yielded a single phase Mg_2SnO_4 in the sintered compacts. Compacts with near zero porosity could be achieved in SSR derived samples up on sintering up to 1600°C, while some significant porosity was an interesting feature of the SHS derived samples. Systematic microstructural evolution with the variation of sintering conditions has been discussed.

Keywords: A. Sintering; B. Electron microscopy; B. X-ray methods; E. Capacitors

1. Introduction

The alkaline–earth stannates having the general chemical formula $MSnO_3$ (M = Ca, Sr and Ba), have recently been studied as potential electronic ceramics, such as, thermally stable capacitors with low permittivity and small loss tangent [1–6]. Interestingly, even though magnesium is a member of the alkaline–earth metal group to which Ca, Sr and Ba belong, no reliable technical information on the electrical behavior of the compounds in the pseudobinary MgO–SnO_2 system appears to exist in the published literature. Limited amount of literature is available on the synthesis aspects of compounds in Mg–Sn–O system. Only P–T relationship has been reported in the literature; no reliable composition–temperature phase diagram exists [7]. On the other hand, corresponding titanates ($MgTiO_3$, Mg_2TiO_4 and $MgTi_2O_5$) and silicates ($MgSiO_3$, steatite and Mg_2SiO_4, forsterite) are commercially produced as low dielectric constant, high resistance and low temperature coefficient of dielectric constant (TCK) components [8]. In addition, the behavior of magnesium metastannate ($MgSnO_3$) and orthostannate (Mg_2SnO_4) is totally different from the corresponding Ca, Sr and Ba counterparts.

Consequently, the literature deals with the thermodynamic stability of the orthostannate alone, albeit with large differences in the computed values of the standard enthalpy of formation of the double oxide from one research to another [9–12]. In addition, the JCPDS files show the presence of another phase with nominal formula $M_3Sn_2O_7$ in all the MO–SnO_2 systems except for Mg. The meta- and orthostannates of calcium, strontium and barium are known to be stable independently up to very high temperatures without disproportionation. $MgSnO_3$ is unstable and disproportionates into orthostannate and tin oxide upon heating above ~700°C. In some cases, even the orthostannate cannot be synthesized as a single-phase [13].

No correlation has been established among key parameters, such as, synthesis, processing, microstructure and electrical behavior of these materials; such a corre-

* Corresponding author at current address: NexTech Materials, Ltd, 720-I Lakeview Plaza Blvd, Worthington, OH 43085, USA. Tel.: +1-614-842-6606; fax: +1-614-842-6607.

E-mail addresses: azad@nextechmaterials.com (A.-M. Azad).

0272-8842/01/$20.00
PII: S0272-8842(00)00085-7

lation is inevitable in understanding the underlying working mechanisms in the electrical components made out from them. In view of the information gaps in the reported research and interesting electrical properties envisaged in magnesium stannates, akin to those in the corresponding silicates and titanates, preliminary yet vigorous and systematic investigations were carried out in $MgO–SnO_2$ system. The results of these detailed investigations are presented in this paper with emphasis on material synthesis, phase relationship and microstructural features of the sintered bodies.

2. Experimental

2.1. Sample preparation

Metallic Sn (99.999% powder, Pi-Kem, Surrey, UK), SnO_2 (99.995% powder, Aldrich, USA), MgO (99.99% powder, BDH, Poole, UK) and $Mg(NO_3)_2{\cdot}6H_2O$ (99% deliquescent crystals, BDH, Poole, UK) were used as the starting materials. The samples investigated in this work were synthesized via two techniques, viz., the traditional solid-state reaction (SSR) route, and a novel method called the self-heat-sustained (SHS) route. Details of these preparative methods with respect to the synthesis of calcium, strontium and barium metastannates have recently been reported elsewhere [1,2]. However, a brief description of these techniques for the synthesis of compounds in $MgO–SnO_2$ system is given here.

2.1.1. Solid-state reaction (SSR) route

Two molar ratios (1:1 and 2:1) of the starting materials, viz., magnesium oxide (or nitrate) and tin oxide were used. The idea was to: (i) explore the possibility of the synthesis of both $MgSnO_3$ and Mg_2SnO_4 as pure single phases, and (ii) unequivocally establish the chemical state of the material in the final sintered product. The stoichiometric quantities (1:1 or 2:1 molar ratio) of MgO or $Mg(NO_3)_2{\cdot}6H_2O$ and SnO_2 powder of stated purity were accurately weighed and dry mixed in an agate mortar. Each of the two mixtures was then separately ball-milled for 4 h in airtight polystyrene bottles using acetone (AR grade, Hamburg Chemicals, India) as a liquid medium and clean zirconia balls as the milling media. The slurry was dried first at room temperature in a ventilated fume hood and then in an air oven. The dried mass was crushed and pulverized in an agate mortar and pestle to fine powder and calcined at different temperatures ranging between as low as 600 to 1300°C for various duration. After each calcination step, the powders were subjected to phase analysis using powder X-ray diffraction at room temperature using CuK_α radiation ($\lambda = 1.5406$ Å) in the range 10–80° (2-θ) to confirm the formation of the targeted compound as a single phase. This was evidenced by the presence of all the diffraction lines corresponding to the targeted compound. The resulting X-ray diffraction (XRD) pattern was also used to detect the presence of, if any, unreacted starting materials and/or phase. In some cases, XRD was also performed on sintered discs in order to confirm that the chemical composition remained unaltered.

The calcined powder was subjected to sintering (in order to follow the evolution of microstructure and its effect on the measured electrical properties) at 1200–1600°C, for soak time ranging between 2 to 48 h in ambient air. Prior to sintering, the calcined powder was blended with polyvinyl alcohol (aqueous solution containing 0.04 g/ml PVA) as a binder, dried overnight and pressed into discs of 10 mm diameter and 1–2 mm thick by uniaxial pressing at pressures not exceeding 100 MPa.

One of the intentions of present investigation was to focus at the most appropriate sintering schedule(s) that would yield a microstructure most benign for the anticipated application of these materials as electronic components. Microstructural features of the starting green powders as well as the sintered discs were determined by using a JEOL-6400SM (Japan) scanning electron microscope (SEM). In the case of powder, the specimen was evenly sprinkled on the glued surface of an aluminum stub. In the case of sintered samples, the specimen were fractured and mounted on aluminum or brass stub without polishing or etching, so as to expose the fractured surface to the incident electron beam in the microscope. Microscopic images were also collected on as-sintered surfaces so as to discern non-uniformity, if any, of grain growth, intergranular connectivity and porosity in the bulk and the surface. Polaron Coating Machine (UK) evaporated a uniform thin film of gold on the exposed surfaces to avoid electrostatic charging during microscopic viewing. The thickness of the gold coating was estimated to be between 10 to 30 Å from the rate and time of evaporation. The calcined powders as well as the sintered discs were stored in the humidity-free bottles containing anhydrous $CaCl_2$, unless required for X-ray analyses or microscopic viewing.

2.1.2. Self-heat-sustained (SHS) reaction route

In this route, MgO powder or $Mg(NO_3)_2{\cdot}6H_2O$ crystals were mixed with metallic Sn in 1:1 and 2:1 molar ratios in an agate mortar and pestle for 1 h. Each mixture was placed in an alumina boat and first heated slowly to and maintained at 250°C for 4 h so as to facilitate complete melting of metallic Sn (melting point = 232°C) and its uniform dispersion under gravitational flow in the liquid state. The temperature was then raised gradually to 800°C and maintained for another 4 h to cause the reaction between molten and free flowing tin and MgO or $Mg(NO_3)_2{\cdot}6H_2O$. The mixture was next calcined at 1100°C for 12 h. The entire

process was carried out in the static ambient air at atmospheric pressure. The attempt to obtain a pure single phase necessitated further heating of the mixture at 1200°C for 24 and 48 h. The calcined mass was crushed, pulverized, mixed with PVA, and sintered according to the *T–t* profile adopted in the case of solid-state derived samples. The details of X-ray analyses and microscopic examination of SHS derived samples remain identical to those described for SSR derived ones.

3. Results and discussion

It should be pointed out that the idea of adopting various synthesis processes was two-fold. First, the limited amount of literature available on the synthesis of magnesium stannates involves SSR route that is presumed to be a conventional method [9,11,12]. Second, it was intended to find a favorable synthesis technique in terms of the phase purity and benign microstructure in the sintered samples with desired electrical characteristics. Paff [13] described a peroxide precursor method to synthesize both $MgSnO_3$ and Mg_2SnO_4. A peroxo precursor is formed via a precipitation step from aqueous solutions of $MgCl_2{\cdot}6H_2O$ and $SnCl_4$, which up on calcination yielded the final compound(s). It was shown that $MgSnO_3$ is formed after thermal degradation of the corresponding peroxo-precursor at temperature below 700°C. Further heating above 700°C led to its decomposition into Mg_2SnO_4 and SnO_2. On the other hand, the thermal decomposition of the X-ray amorphous precursor with 2:1 (Mg to Sn) molar ratio, led directly to Mg_2SnO_4 formation at 900°C and above.

3.1. X-ray diffraction of solid-state reaction derived samples

Fig. 1 shows the diffraction patterns in the (1:1) powder mixtures of MgO (or $Mg(NO_3)_2$) and SnO_2 calcined at temperatures of 600 to 1300°C for duration ranging between 3 to 48 h. It can easily be seen that the XRD signature of the powder calcined up to 800°C is quite different from those calcined at higher temperatures. Apparently, $MgSnO_3$ is unstable above 800°C and disproportionates into Mg_2SnO_4 and SnO_2. Comparison of the XRD lines with the JCPDS standard cards (24-0723 and 41-1445) showed progressive increase in the amount of Mg_2SnO_4 with increase in calcination temperature and time. The most salient feature of Fig. 1 is that the end product of a 1:1 molar mixture of the starting material is ultimately a two-phase mixture irrespective of the calcination conditions. Moreover, the lines characteristic of the orthostannate phase begin to appear in the XRD signature of the powder calcined at as low as 800°C. This result is in excellent agreement

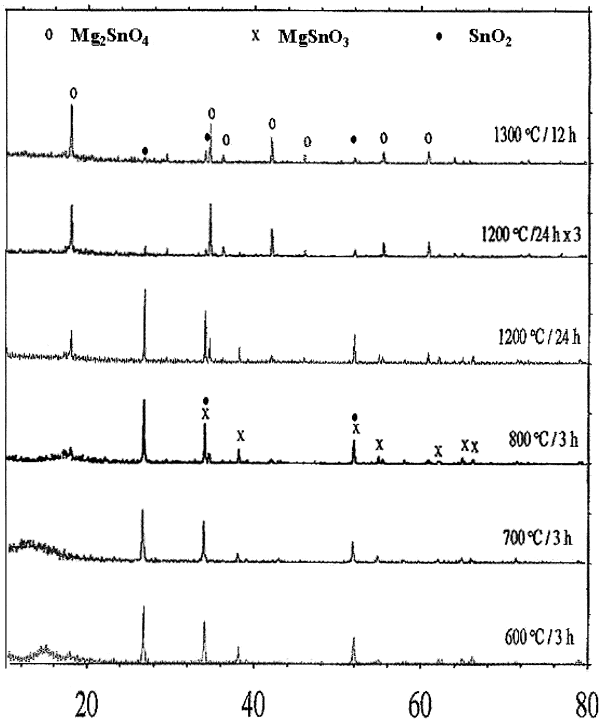

Fig. 1. The XRD patterns of the powders obtained via solid-state reaction (SSR) between magnesium oxide and tin oxide in 1:1 molar mixtures under various calcination conditions.

with those of Pfaff [13]. The appearance of very sharp diffraction peaks further indicates the presence of very small crystallite size in the calcined powders. In the light of X-ray data presented in Fig. 1, one can speculate that the formation of $MgSnO_3$ initially, and subsequently of Mg_2SnO_4 with SnO_2, in 1:1 molar mixtures of the starting precursors takes place in the following manner:

At low temperatures ($T \leqslant 800$°C):

$$MgO \text{ or } Mg(NO_3)_2 + SnO_2 \rightarrow MgSnO_3 \quad (1)$$

At high temperatures ($T > 800$°C):

$$MgSnO_3 \rightarrow 0.5\ Mg_2SnO_4 + 0.5\ SnO_2 \quad (2)$$

As for the samples derived from 2:1 molar mixtures, the XRD results show that the final phase in powders obtained after calcination at 1200°C for 12 h consisted predominantly of the orthostannate phase, viz., Mg_2SnO_4, with small peaks corresponding to the SnO_2. The XRD pattern of powder compacts sintered at 1500°C/6 h and 1600°C/2 h, however, corresponded to that of pure Mg_2SnO_4 phase without even traces of other compound(s). This is illustrated in Fig. 2, where the diffractograms of calcined and sintered bodies are compared. Thus, it appears that while in 1:1 mixtures formation of the orthostannate phase invariably goes via the formation and disproportionation of metastannate ($MgSnO_3$), latter forms more or less directly in

2:1 molar mixtures. Small amounts of SnO_2 observed in calcined powders, however, suggest that some $MgSnO_3$ might have formed in the initial stages as a result of parallel reactions of the type shown below:

$$MgO + SnO_2 \rightarrow MgSnO_3 \quad (3)$$

$$2\ MgO + SnO_2 \rightarrow Mg_2SnO_4 \quad (4)$$

The systematic variation in the relative amounts of magnesium orthostannate and tin oxide in the mixtures with two stoichiometries, calcined in the range 1200–1300°C for various duration, is presented in Fig. 3 in terms of the intensity ratio (I/I_o) of the most prominent peaks. In both the cases it can be seen that, as the calcination temperature and time increased, Mg_2SnO_4 became more prominent with corresponding decrease in the amount of SnO_2. The intensity of Mg_2SnO_4 in 2:1 sample in greater than in 1:1 sample. This is due to the fact that the direct formation of Mg_2SnO_4 is favored in 2:1 molar mixture as mentioned above.

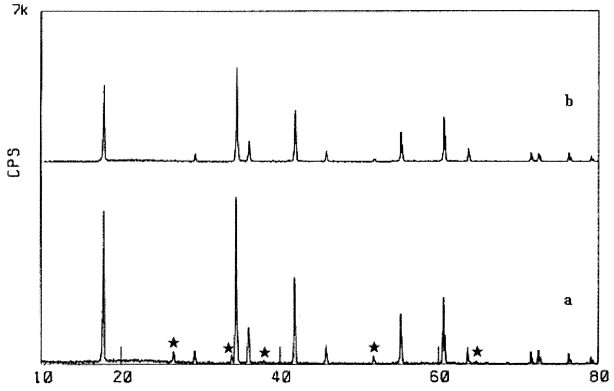

Fig. 2. Comparative XRD signatures of 2:1 mixtures: (a) powder calcined at 1200°C/12 h and (b) sintered pellet at 1500°C/6 h. (⋆: SnO_2.).

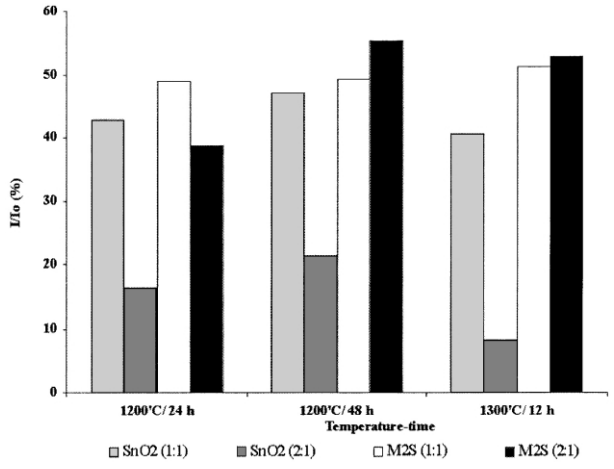

Fig. 3. Relative variation of Mg_2SnO_4 and SnO_2 in samples derived via solid-state reaction (SSR) technique under different conditions.

3.2. X-ray diffraction of SHS reaction derived samples

The SHS technique makes use of the low melting characteristic of metallic tin. It is envisaged that when liquid tin mixes with MgO or $Mg(NO_3)_2$ under gravitational flow, it forms $MgSnO_3$ first. Subsequently at higher temperatures, due to its instability, $MgSnO_3$ decomposes into Mg_2SnO_4 and SnO_2. The XRD signatures of 1:1 molar mixtures of powders synthesized via SHS techniques at various temperatures ranging between 1100 to 1300°C for 12 to 48 h showed that the final chemical state in the 1:1 molar mixture, in the case of SHS technique as well, consists of a two-phase mixture of Mg_2SnO_4 and SnO_2. As discussed in the case of SSR-derived samples (Fig. 1), this could be the result of decomposition of $MgSnO_3$ formed at lower temperature. The reaction pathway for the formation of Mg_2SnO_4 and SnO_2 in a 1:1 molar mixture via SHS technique could be visualized as follows:

At low temperatures:

$$MgO \text{ or } Mg(NO_3)_2 + Sn(metal) + O_2(g) \rightarrow MgSnO_3 \quad (5)$$

and

$$2\ MgO \text{ or } 2\ Mg(NO_3)_2 + Sn(metal) + O_2(g) \rightarrow Mg_2SnO_4 \quad (6)$$

At high temperatures:

$$MgSnO_3 \rightarrow 0.5\ Mg_2SnO_4 + 0.5\ SnO_2 \quad (2)$$

In accordance with the reactions represented by Eqs. (2), (5) and (6), Mg_2SnO_4 was found to be the majority phase with SnO_2 as the minor impurity in the calcined powders. With gradual increase in calcination temperature and/or time, there was a steady decrease in the

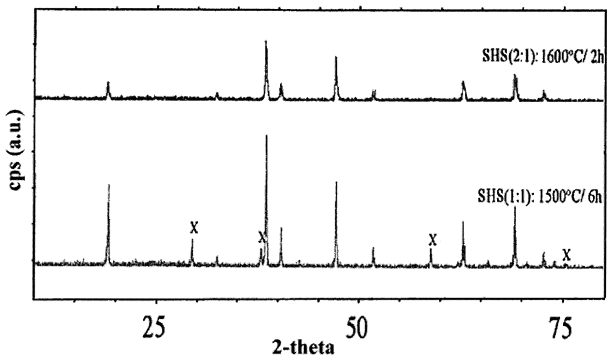

Fig. 4. Nature of phase existence in 1:1 and 2:1 mixtures derived via self-heat-sustained (SHS) technique up on sintering at high temperatures. (X: SnO_2.).

amount of SnO_2, and, the sample calcined at 1300°C comprises of pure Mg_2SnO_4. The X-ray signatures of the compacts sintered up to 1500°C for 6 h and 1600°C for 2 h, show a two-phase mixture ($Mg_2SnO_4 + SnO_2$) and a pure phase (Mg_2SnO_4) in the 1:1 and 2:1 mixture, respectively (Fig. 4).

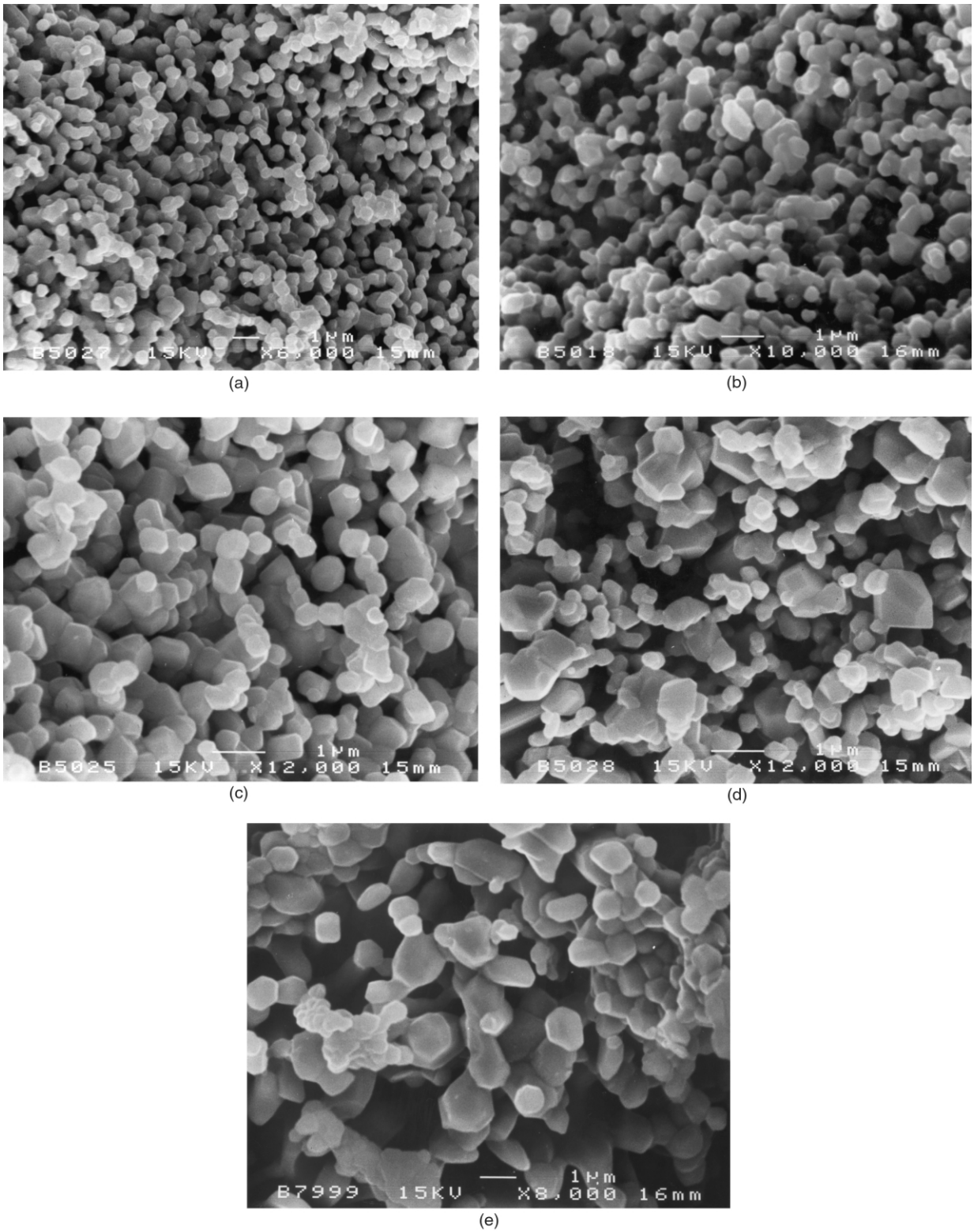

Fig. 5. Morphology of powders calcined at 1200°C/24 h with: (a) $MgO + SnO_2$ (1:1), (b) $Mg(NO_3)_2 + SnO_2$ (1:1), (c) $Mg(NO_3)_2 + SnO_2$ (2:1), (d) $Mg(NO_3)_2$ + metallic Sn (1:1) and (e) $Mg(NO_3)_2$ + metallic Sn (2:1); (a–c): solid-state reaction (SSR), (d–e): self-heat-sustained (SHS) technique.

3.3. Microstructural features of the calcined samples

The morphological features of the solid-state derived green powders with different starting materials (i.e. oxide or nitrate of magnesium) in two different molar ratios, are shown in Fig. 5(a–c). The grain size in the calcined powder is uniform and very small (submicron level) crystallites with a narrow particle size distribution can easily be recognized. Thus the powder is quite reactive; such benign features are helpful in minimizing the possibility of abnormal grain growth and increasing the densification up on subsequent sintering. Another interesting feature of these materials is that the morphology of the powders is almost identical in all the cases and therefore, gives a free choice of selecting the starting precursors for material synthesis. In contrast, the morphology of the powders derived from SHS technique is quite different from that observed in SSR-derived ones. The microstructures shown in Fig. 5(d–e) for SHS samples after calcination at 1200°C for 24 h clearly bring out the difference, as the granular (crystallized) nature of the particles can be easily made out. The average grain size in the 1:1 molar mixture is less than 1 μm with broader particle size distribution [Fig. 5 (d)], while that in the 2:1 mixture is ~1 μm and rather more uniform [Fig. 5 (e)]. This could be attributed to the envisaged scheme by which reactions in the two mixtures take place, the formation of magnesium orthostannate being direct in the case of higher Mg:Sn ratio.

3.4. Microstructural evolution in sintered bodies

The X-ray analyses presented in the preceding section have amply demonstrated that magnesium orthostannate is formed in pure form in 2:1 and with SnO_2 as a minor secondary impurity phase in the 1:1 molar mixtures of the magnesium and tin precursors. Accordingly, there are certain differences in the microstructural artifacts of the sintered bodies of the two kinds. To maintain clarity of presentation, the microstructural

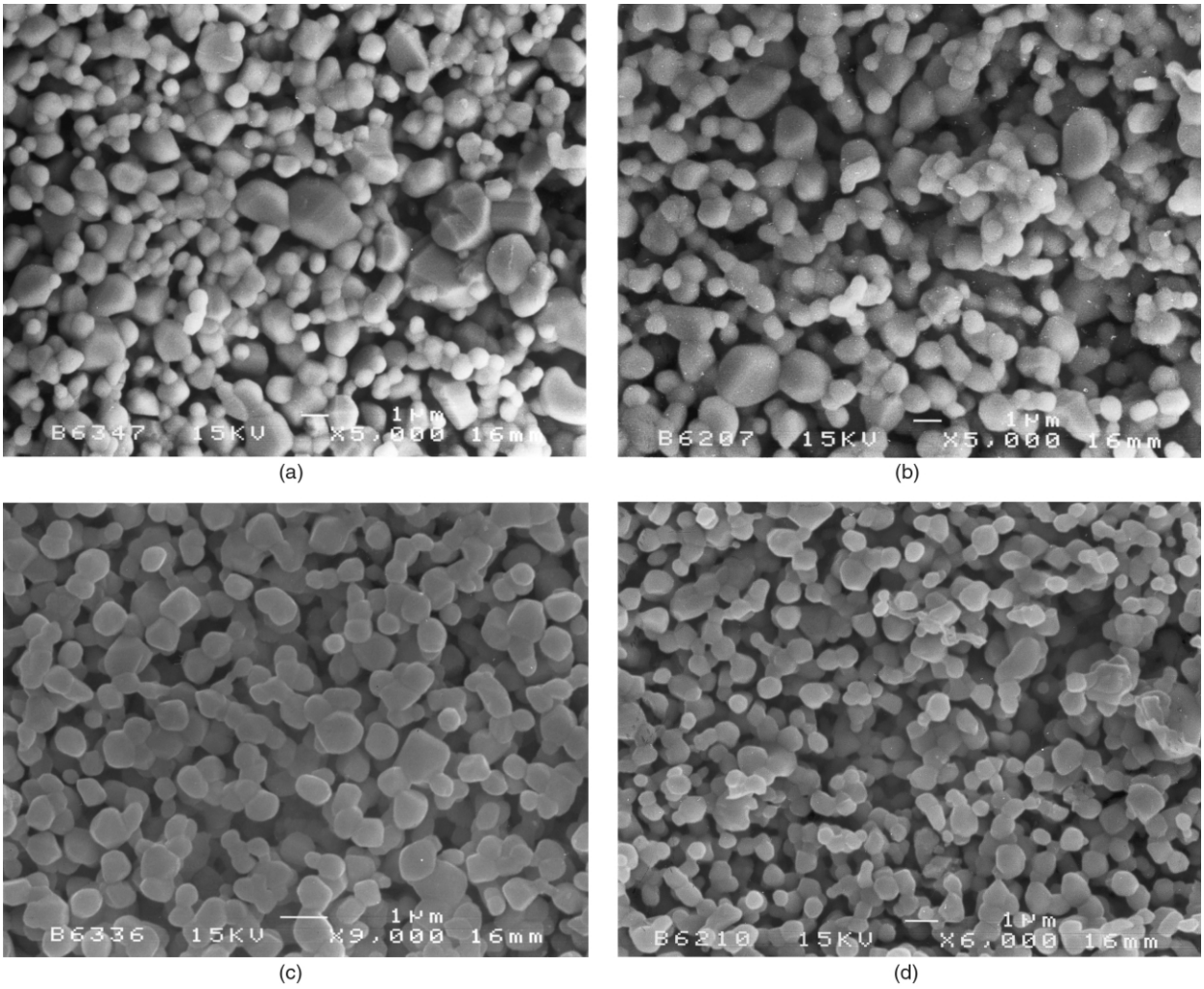

Fig. 6. Microstructural features of solid-state reaction (SSR) derived samples sintered at 1200°C and soaked for (a) 24 h/1:1 (b) 48 h/1:1 (c) 24 h/2:1 and (d) 48 h/2:1.

features will be discussed sequentially according to the technique of powder synthesis as well as with respect to the molar ratios of the two cations in the calcined powders.

3.5. SSR-derived compacts

Fig. 6 shows the microstructural features in solid-state derived samples sintered at 1200°C for 24 and 48 h. As can be seen, the sample is quite porous but majority of the grains are in the size range of 0.2–0.5 μm. It can also be seen that the grain size distribution is narrower in the sintered bodies with Mg to Sn ratio equal to 2:1. However, the setting-in of intergranular connectivity that eventually leads to densification in solids is evident. Moreover, the morphological similarities indicate that the sintering process was uniform throughout the samples. The samples sintered at 1300°C for 24 h showed evidence of grain growth, improved grain-to-grain connectivity and marked decrease in porosity (Fig. 7). In addition, there was a definite reduction in grain size distribution with improved densification, particularly in the 2:1 mixtures. With further increase in sintering temperature to 1400°C, further grain growth leading to still better intergranular connectivity with clean grain boundaries and reduced porosity was achieved (Fig. 8). These benign features are a consequence of enhanced diffusion and mass transport at higher temperature and longer soak time.

The microstructural evolution in samples soaked for 2 h at 1600°C shown in Fig. 9, brings out the remarkable increase in grain growth and intergranular contact in both sets of samples. However, while almost zero porosity in 2:1 samples sintered at 1600°C/2 h can be clearly seen, pores could not be eliminated effectively in 1:1 mixtures sintered under identical conditions. It is likely that at such high temperatures, evaporation of SnO_2 (detected as a minor impurity phase) as per the reaction:

$$SnO_2(s) \rightarrow SnO(g) + 1/2\ O_2(g) \quad (7)$$

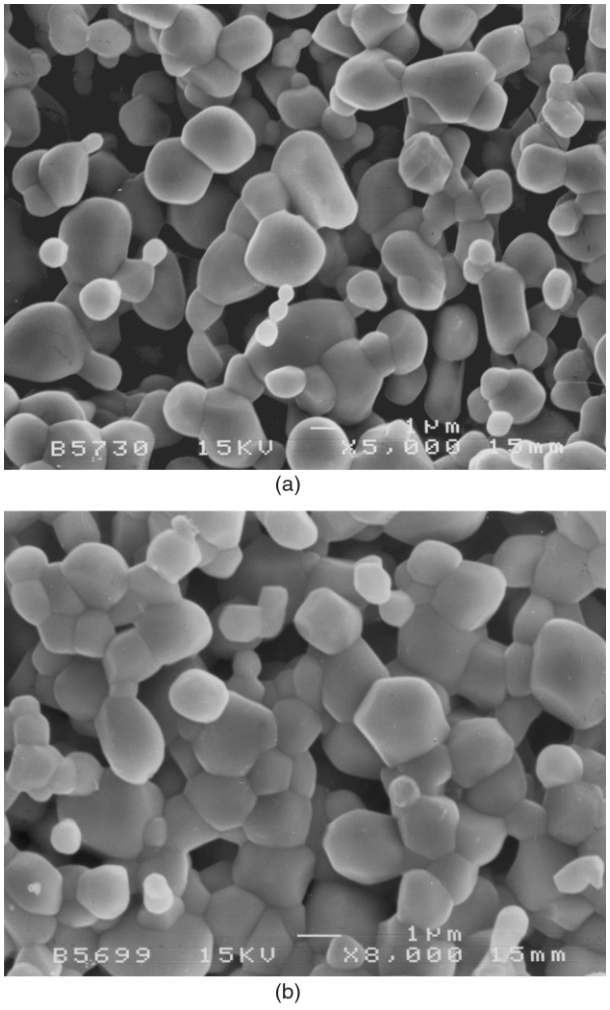

Fig. 7. Microstructural development in compacts soaked at 1300°C/24 h: (a) 1:1 and (b) 2:1 molar mixture.

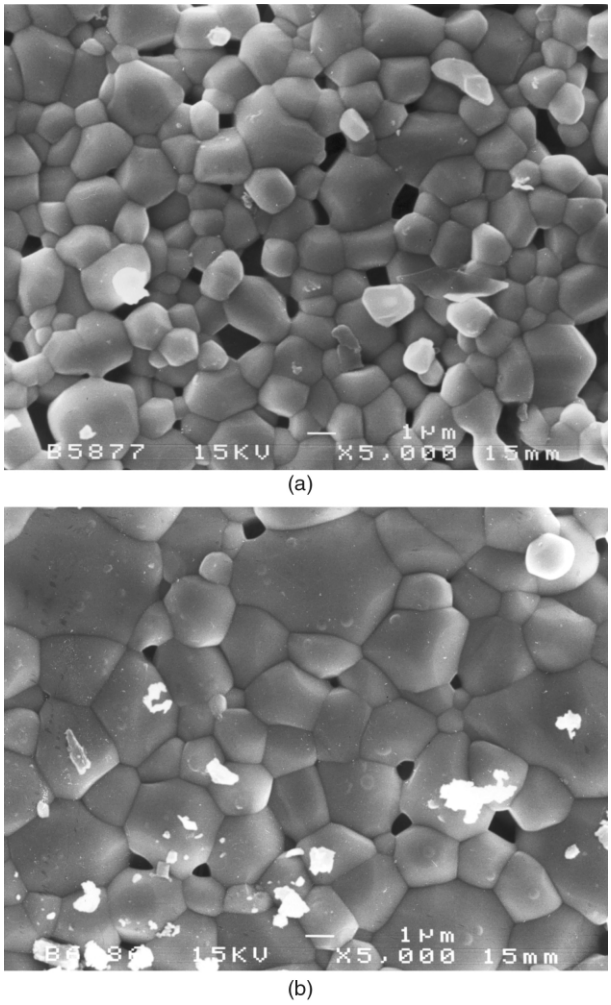

Fig. 8. Evolution of microstructure in 2:1 compact sintered at 1400°C for: (a) 6 h and (b) 12 h.

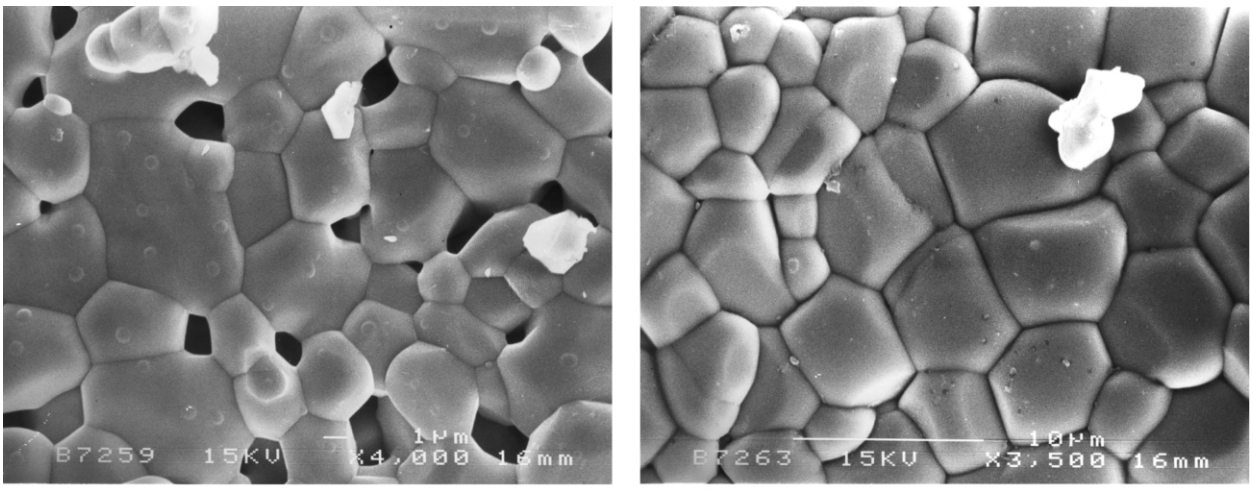

Fig. 9. Microstructural artifacts of samples sintered at 1600°C/2 h in: (a) 1:1 and (b) 2:1 molar mixtures.

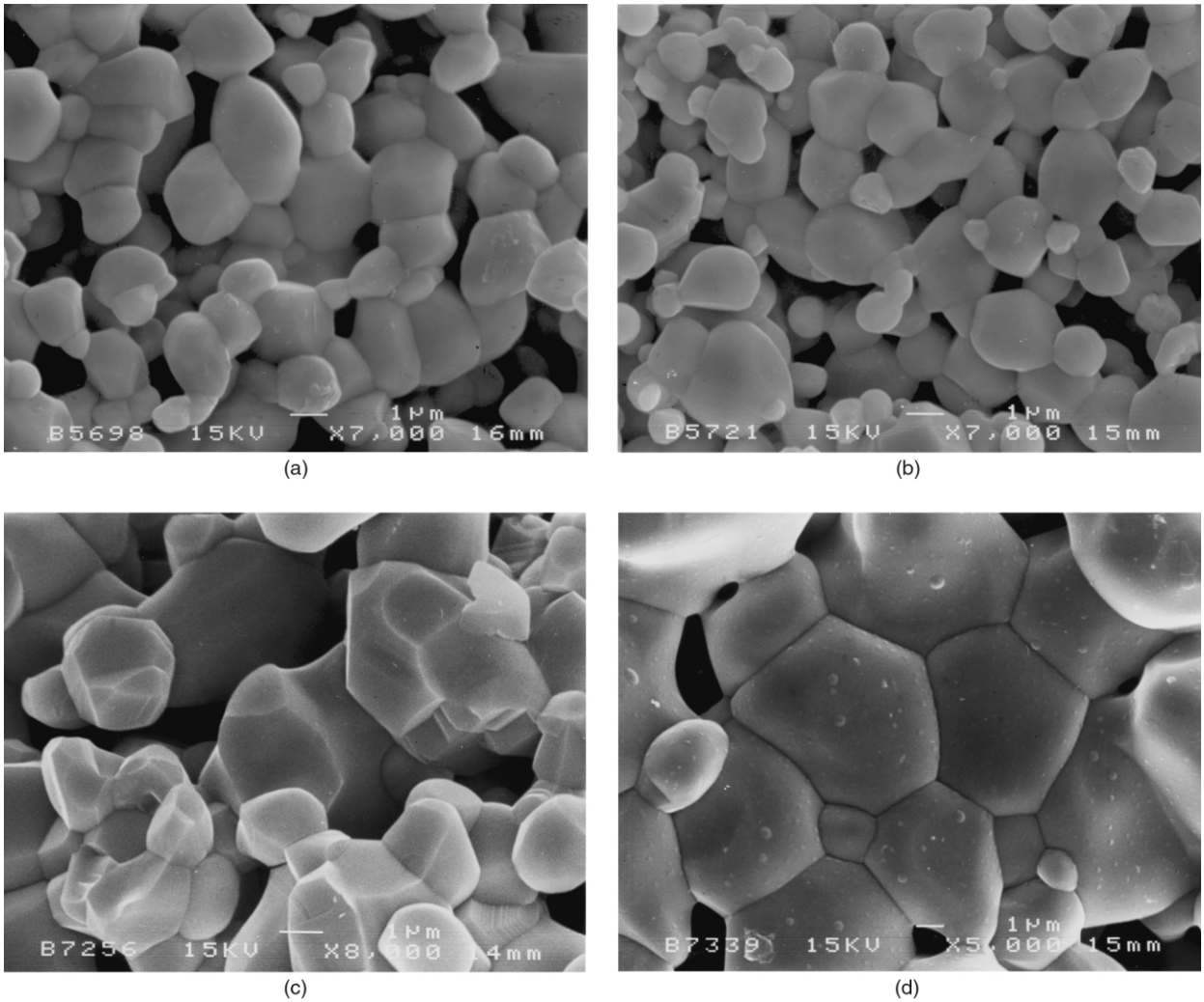

Fig. 10. Microstructural features in self-sustained-heat (SHS) samples: (a) soaked for 24 h at 1300°C (1:1), (b) soaked for 24 h at 1300°C (2:1), (c) soaked for 6 h at 1500°C (1:1), fractured surface and (d) soaked for 2 h at 1600°C (2:1).

could have led to the observed porosity. Thus while a small fraction porosity still exists in 1:1 mixtures, near theoretical density could be achieved in samples derived with 2:1 molar mixtures. Nevertheless, the remnant porosity even in the sintered bodies of 1:1 mixtures is isolated in nature and in fact, did not impart any visible detrimental effect on the electrical characteristic of the material, as discussed in the subsequent paper [14].

3.6. SHS-derived compacts

The microstructures evolved in the samples derived via SHS technique and sintered at 1200°C for 24 and 48 h did not show any grain growth and hence this temperature-time schedule was inadequate for meaningful sintering. The samples remained highly porous with particle size distribution being rather broad in 1:1 mixtures compared to that in the 2:1 mixtures. This behavior is akin to that in SSR-derived samples sintered under identical conditions (Fig. 6). The average grain size in the 1:1 molar mixtures ranged from submicron to ~1 μm while that in 2:1 mixture remained close to 1 μm. Sintering at 1300°C for 24 h did help in causing grain growth to some extent (average grain size >1 μm) in both 1:1 and 2:1 molar ratio compacts, as shown in Fig. 10(a and b). Porosity, however, still remained high (being higher in 1:1 mixtures). In addition, the particle size distribution was narrower in samples with magnesium to tin ratio 2:1.

As it is well known, one of the major limitations of SHS synthesis is the presence of relatively higher degree of porosity in the final product [1,2]. Nevertheless, since about 95% of this porosity is 'open' in nature, it can be eliminated by choosing proper sintering schedule, thereby resulting in a dense and compact body. Accordingly, a systematic increase in grain size, reduction in porosity together with enhanced material densification can be delineated from the microstructural features presented in Fig. 10(c and d) for samples sintered at 1500 and 1600°C for 6 and 2 h, respectively. In samples sintered at 1600°C, some of the grains have grown up to ~5 μm. The similarity in microstructural features of the as-sintered and fractured surfaces was also readily seen in these samples.

4. Conclusions

The following conclusions could be drawn from this study:

1. Magnesium metastannate, $MgSnO_3$, is a low-temperature phase which disproportionates into Mg_2SnO_4 and SnO_2 at or above 800°C. The ultimate phase in the calcined powders synthesized via either of the two techniques with starting composition in 1:1 molar ratios is a mixture of Mg_2SnO_4 and SnO_2. In the case of 2:1 molar mixtures, Mg_2SnO_4 is formed as a single phase with 1–2 peaks of SnO_2 as a minor impurity phase that disappears up on treatment at higher temperatures. The sintered bodies (at 1500°C/6 h and 1600°C/2 h) with 2:1 ratio of Mg to Sn indicate the presence of orthostannate alone, irrespective of the preparative technique employed. In the case of powders synthesized via SHS technique, the XRD signatures of the sintered bodies (up to 1600°C/2 h) indicate that the final chemical state is Mg_2SnO_4 in 2:1 and predominantly Mg_2SnO_4 with SnO_2 in 1:1 mixtures.
2. The average grain size was less than or about 1 μm in calcined powders derived via SSR and SHS route, respectively. Highly dense bodies with near zero porosity could be obtained by sintering the SSR-derived powder compacts (2:1) at 1600°C for 2 h. Porosity, however, could not be fully eliminated in compacts of SHS derived powders (both 1:1 and 2:1) sintered up to 1600°C. Density was higher in SSR derived samples than in their SHS counterparts, sintered at a given temperature.
3. In the case of SSR route, better densification was achieved in the 2:1 molar mixtures at higher temperatures. This could be explained in terms of evaporation loss of SnO_2 present as an impurity phase in 1:1 mixtures leaving behind slightly porous body. Since Mg_2SnO_4 is formed directly in the 2:1 mixtures, there is no such loss and therefore less or no porosity is envisaged and observed. The microstructural artifacts evolved in the compacts of SHS derived powders sintered up to 1600°C/2 h suggested that both the samples with magnesium to tin ratio 1:1 and 2:1 achieved very high densification, narrower particle size distribution and reduced porosity.

Acknowledgements

The authors are indebted to Associate Professor Mansor Hashim for his keen interest and constant encouragement during the course of this work and to the staff of the Electron Microscopy Unit of the Institute of Bioscience, University Putra Malaysia for allowing the extensive use of the JEOL Electron Microscope and its accessories.

References

[1] A.-M. Azad, N.C. Hon, J. Alloys Comp. 270 (1998) 95.
[2] A.-M. Azad, L.L.W. Shyan, P.T. Yen, J. Alloys Comp. 282 (1999) 109.
[3] A.-M. Azad, L.L.W. Shyan, P.T. Yen, N.C. Hon, Ceram. Int. 26 (2000) 685.

[4] A.-M. Azad, L.L.W. Shyan, M.A. Alim, J. Mater. Sci. 34 (1999) 1175.
[5] A.-M. Azad, L.L.W. Shyan, M.A. Alim, J. Mater. Sci. 34 (1999) 3375.
[6] A.-M. Azad, T.Y. Pang, M.A. Alim, Smart Mater. Struct. 2000 (in press).
[7] A.E. Ringwood, Earth Planet. Sci. Lett. 5 (1968) 245.
[8] J.M. Herbert, Ceramic Dielectrics and Capacitors, Gordon and Breach Science Publishers, Philadelphia, 1985.
[9] I.N.S. Jackson, R.C. Liebermann, A.E. Ringwood, Earth Planet. Sci. Lett. 24 (1974) 203.
[10] A. Navrotsky, R.P. Kasper, Earth Planet. Sci. Lett. 31 (1976) 247.
[11] K.T. Jacob, J. Valderrama-N, J. Solid State Chem. 22 (1977) 291.
[12] S. Raghavan, Thermochim. Acta 122 (1987) 389.
[13] G. Pfaff, Thermochim. Acta 237 (1994) 83.
[14] A.-M. Azad, L.J. Min, M.A. Alim, This work (part II), Ceram. Int. 27 (2000) 335.